Journal of Magnetic Resonance 211 (2011) 243–247

Contents lists available at ScienceDirect

Journal of Magnetic Resonance

journal homepage: www.elsevier.com/locate/jmr

Communication

Exchange enhanced sensitivity gain for solvent-exchangeable protons in 2D ^{1}H–^{15}N heteronuclear correlation spectra acquired with band-selective pulses

Shenggen Yao [a,b,*], Mark G. Hinds [a,b,c], James M. Murphy [a,b], Raymond S. Norton [d]

[a] The Walter & Eliza Hall Institute of Medical Research, 1G Royal Parade, Parkville, Victoria 3052, Australia
[b] Department of Medical Biology, The University of Melbourne, Parkville, Victoria 3010, Australia
[c] Bio21 Institute, The University of Melbourne, Parkville, Victoria 3010, Australia
[d] Monash Institute of Pharmaceutical Sciences, Monash University, Parkville, Victoria 3052, Australia

ARTICLE INFO

Article history:
Received 31 March 2011
Revised 12 May 2011
Available online 31 May 2011

Keywords:
Band-selective excitation
BEST
Heteronuclear correlation spectroscopy
Sensitivity enhancement
SOFAST-HMQC
Solvent-exchangeable protons

ABSTRACT

Conformational or chemical exchange can cause significant sensitivity loss in NMR spectroscopy through resonance broadening for nuclear spins involved in these processes. While this effect may sometimes be alleviated by manipulating experimental conditions such as temperature, pH, and buffers, conditions optimal for all resonances are not always achievable. As a consequence, any means of recovering or minimizing this exchange-induced sensitivity loss is potentially of significant value in regaining information otherwise lost. We report the experimental observation of significant sensitivity gain for nuclear spins undergoing chemical exchange with solvent (water) at exchange rates ca 1–10 s^{-1} in ^{1}H–^{15}N correlation spectra of proteins acquired with band-selective pulses (the SOFAST-HMQC sequence).

1. Introduction

Spectral line broadening and subsequent disappearance of resonances are often encountered in NMR spectra of biomolecules as a consequence of chemical or conformational exchange on the timescale of microseconds to milliseconds. Conditions optimal for all nuclear spins in a given sample are not always readily achievable, even after exhaustive experimental manipulation of temperature, pH, and buffers [1]. Any means of recovering/minimizing this sensitivity loss would therefore be of value in regaining information otherwise lost. Dedicated schemes incorporated into the TROSY (*T*ransverse *R*elaxation-*O*ptimised *S*pectroscop*Y*) version of the ^{1}H–^{15}N HSQC (*H*eteronuclear *S*ingle *Q*uantum *C*oherence) sequence have been developed recently for suppression of the line broadening induced by conformational exchange using "chemical shift scaling" [2,3]. It has also been shown that protonless (^{13}C-detected) NMR spectroscopy can be used to alleviate the loss of information due to exchange broadening [4]. In contrast to line broadening resulting from conformational exchange, sensitivity loss arising from backbone amide proton exchange with solvent (normally water) is usually not as deleterious as that caused by local conformational heterogeneity because backbone amide protons undergoing exchange with water are usually in the slow exchange regime (relative to the chemical shift timescale) [5]. More often these exchanging amide protons are also located in or near the conformationally flexible regions of proteins, such as the N- and C-termini or long loops where local flexibility gives rise to relatively longer transverse relaxation times and effectively compensates the potential loss of sensitivity resulting from exchange with the solvent to some extent. Significant sensitivity loss may occur, however, when the exchange deviates from the slow exchange regime; in extreme situations backbone amides in rapid exchange with water may be unobservable [6].

The SOFAST-HMQC (band-*S*elective *O*ptimized *F*lip-*A*ngle *S*hort-*T*ransient *H*eteronuclear *M*ultiple *Q*uantum *C*oherence) sequence [7], is one of several methods that have been introduced to achieve sensitivity enhancement in NMR spectroscopy by speeding up the acquisition of multi-dimensional NMR spectra [8–12]. The SOFAST-HMQC sequence employs the BEST, *B*and-selective *E*xcitation *S*hort *T*ransient, scheme [13] to achieve longitudinal relaxation optimization for backbone amide protons, allowing short relaxation delays (inter-scan delay, T_R) between scans (typically $\leqslant$100 ms) without saturating amide proton magnetization [7]. Consequently, it significantly improves the sensitivity of 2D heteronuclear correlation spectra when compared with that of conventional methods such as the sensitivity-enhanced, water-flip-back HSQC sequence [14,15].

The basis of sensitivity enhancement observed in SOFAST-HMQC over the conventional ^{1}H–^{15}N HSQC method is well explained by spin diffusion [12,16]. Band-selective pulses perturb

* Corresponding author at: The Walter & Eliza Hall Institute of Medical Research, 1G Royal Parade, Parkville, Victoria 3052, Australia. Fax: +61 3 93470852.
E-mail address: syao@wehi.edu.au (S. Yao).

1090-7807/$ - see front matter © 2011 Elsevier Inc. All rights reserved.
doi:10.1016/j.jmr.2011.05.013

only the spins of interest (e.g. amide protons), but leave all others (e.g. solvent and aliphatic protons) unperturbed, effectively dividing the spin ensemble into two pools at different spin-temperature [17] with one pool (pool-I) consisting of perturbed spins at higher spin-temperature and the second (pool-II) containing unperturbed spins at lower spin-temperature. The presence of this spin-temperature difference allows the magnetization of spins in pool-II to be transferred to spins in pool-I during the inter-scan delay, T_R, via spin diffusion and/or chemical exchange [18] processes, effectively allowing those excited spins in pool-I to return to their equilibrium states at rates much faster than their intrinsic longitudinal relaxation rates, R_1 [19]. In this communication, we report the experimental observation of significant exchange enhanced sensitivity gain for nuclear spins undergoing relatively rapid chemical exchange with water ($k \sim 1$–$10\ s^{-1}$) in ^1H–^{15}N correlation spectra acquired with the SOFAST-HMQC sequence [7].

2. Results and discussion

Murine interleukin-3 (mIL-3_{33-156}, consisting of residues 33–156 with a single amino acid substitution C105A) [20] contains a group of residues displaying substantial conformational and/or chemical exchange phenomena in solution [21,22]. A number of residues exhibit non-linear temperature dependence, deviating from linearity at higher temperature, for their backbone amide ^1H chemical shifts over the temperature range 283–303 K [22]. In addition, ^{15}N relaxation dispersion measurements revealed a group of residues accessing alternative conformations at 298 K (but not at 283 K), and the amide resonances of N42, K71, and A111 disappeared at higher temperature (>293 K in ^1H–^{15}N HSQC spectra, at 600 MHz) [22]. Conformational exchange has been reported to be responsible for non-linear temperature dependence of backbone amide ^1H chemical shifts [23] and resonances disappearing and reappearing in a temperature-dependent manner was also thought to be the result of conformational averaging between native subpopulations [24,25]. While data from both ^{15}N relaxation dispersion and temperature dependence of backbone amide resonances suggest the presence of local conformational heterogeneity within mIL-3_{33-156} [22], the CLEANEX experiments [26] performed on mIL-3_{33-156} at 283 K (Fig. 1) confirm unambiguously the presence of rapid chemical exchange with water for the backbone amide protons of N42, K71, and A111 at 283 K, with exchange rates of 2.2, 2.1, and 4.5 s^{-1}, respectively, at 283 K compared with exchange rates of 0.6, 0.5, and 1.5 s^{-1}, respectively, for L37, A153, and G155 from the N- and C-termini (see Fig. 1C).

Backbone amide resonances of N42, K71, and A111 are visible at 293 K, but broadened considerably due to chemical exchange with water. At 288 K, their intensities are still significantly lower (particularly for K71) when compared with other resonances such as K97 and R122. Partial ^1H–^{15}N HSQC and SOFAST-HMQC spectra of mIL-3_{33-156} containing resonances of K71, K97, A111, and R122 at 288 and 283 K are shown in Fig. 2. As can be seen from Fig. 2B and D, the SOFAST-HMQC with an inter-scan delay, T_R, of 100 ms yields a peak intensity for K71 comparable with those of K97 and R122 (whose amide protons are not undergoing significant exchange with water) and an intensity for A111 even stronger than those of K97 and R122 (Fig. 2B).

Intensity ratios for amide resonances of mIL-3_{33-156} calculated from their respective resonance intensities in SOFAST-HMQC and ^1H–^{15}N HSQC spectra (283 K) plotted as a function of the inter-scan delay, T_R, used in SOFAST-HMQC are depicted in Fig. 3A. Fig. 3B plots the intensity ratios of SOFAST-HMQC (T_R = 100 ms) and ^1H–^{15}N HSQC vs. their sequence position for mIL-3_{33-156} at 283 K. Significant exchange enhanced sensitivity gains are evident for the amide resonances of N42, K71, and A111 relative to other

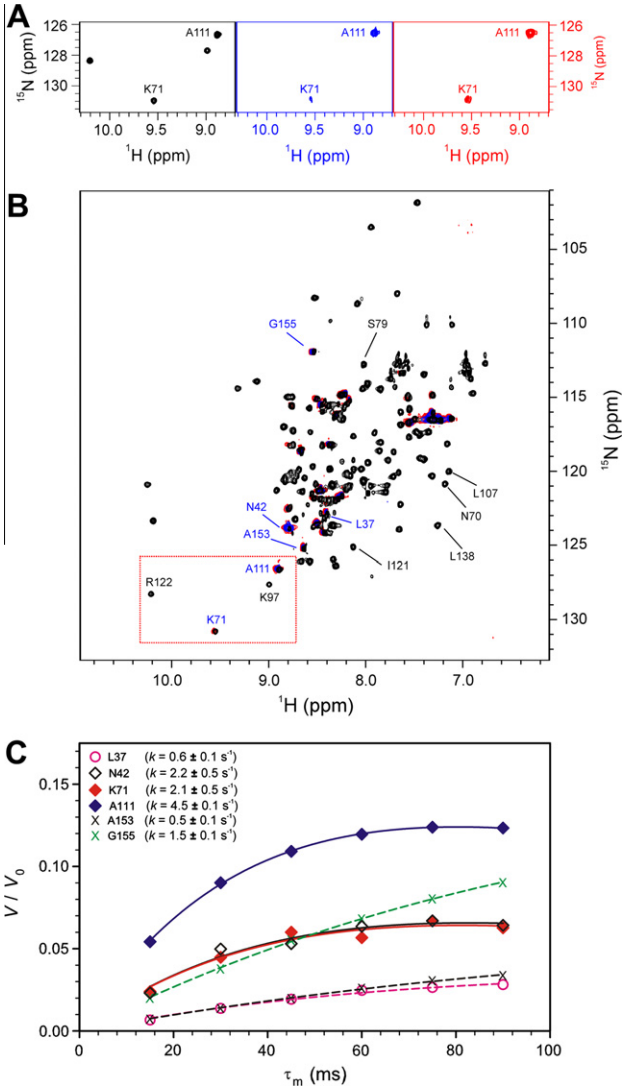

Fig. 1. Amide protons of mIL-3_{33-156} in chemical exchange with water as detected by CLEANEX experiments. (A) Regions of ^1H–^{15}N HSQC (left panel) and CLEANEX spectra (middle and right panels with mixing times of 15 ms and 60 ms, respectively) of mIL-3_{33-156} containing water-exchangeable residues K71 and A111. (B) CLEANEX spectra of mIL-3_{33-156} recoded at 283 K with mixing time of 15 ms (in blue) and 60 ms (in red) superimposed on the ^1H–^{15}N HSQC spectrum with residues shown in Figs. 2C and 3A labelled (residues exhibiting exchange with solvent water at 283 K, as detected by CLEANEX, are labelled in blue, those that do not exhibit exchange with water are labelled in black). (C) Ratios of peak volumes for a group of residues, calculated from CLEANEX spectra at various mixing times and a reference ^1H–^{15}N HSQC spectrum, vs. the mixing time (exchange spinlock) used in the CLEANEX sequence. All lines represent fits to Eq. (1). (For interpretation of the references to colour in this figure legend, the reader is referred to the web version of this article.)

amide resonances, including those of L37, A153 and G155 from the N- and C-termini, which are also in exchange with water. The results shown in Figs. 2 and 3 demonstrate that backbone amides displaying significant exchange enhanced sensitivity gains in SOFAST-HMQC spectra (acquired using band-selective pulses) correlate with those undergoing rapid exchange with water.

Representative backbone amide resonance intensities of mIL-3_{33-156} from conventional ^1H–^{15}N HSQC and SOFAST-HMQC as well as their ratios as a function of temperature are shown in Fig. 4A and B, respectively. As the temperature increases, the exchange of the C-terminal A153 and G155 amide protons with water becomes more efficient and the sensitivity gain from SOFAST-HMQC over conventional ^1H–^{15}N HSQC improves accordingly for these amides. In contrast, for backbone amides not showing significant

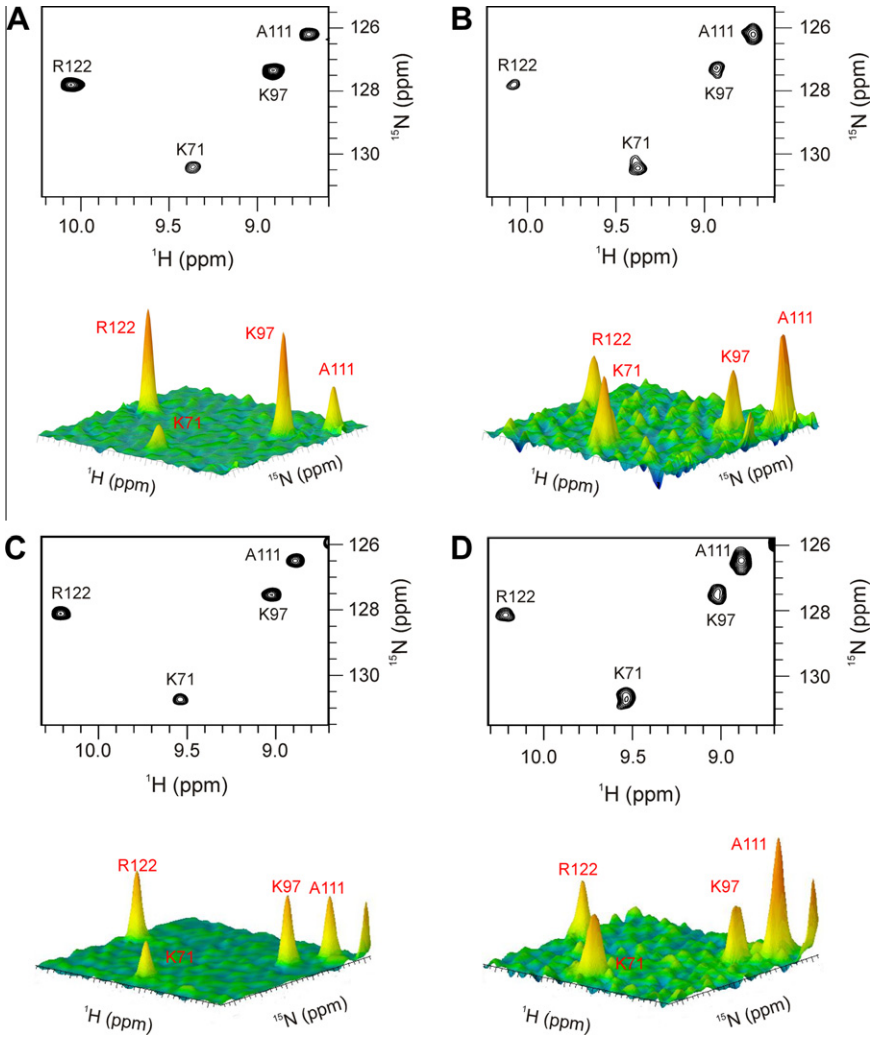

Fig. 2. Exchange enhanced sensitivity gain in SOFAST-HMQC spectra for backbone amide protons in rapid exchange with water. Regions of ^{1}H–^{15}N HSQC and SOFAST-HMQC spectra of mIL-3_{33-156} in contour and stacked plots, showing significant signal gain for K71 and A111 resonances in SOFAST-HMQC at 288 (A and B) and 283 K (C and D). A and C were recorded with the sensitivity-enhanced water-flip-back HSQC sequence, T_R = 1.2 s, 128 transients, total acquisition time 5 h 50 min at 288 and 283 K, respectively. B and D were obtained using a SOFAST-HMQC sequence, T_R = 43.5 ms, 96 transients, total acquisition time 23 min 14 s at 288 and 283 K, respectively.

exchange with the water (K97 and I121) the sensitivity gains at higher temperatures (over the range studied) are minimal. For N42, K71, and A111, on the other hand, as temperature increases the sensitivity gain from SOFAST-HMQC also rises, but, at temperatures $\geqslant$293 K, these amide resonances become too weak to detect even in SOFAST-HMQC under the present conditions (with a total acquisition time of ~23 min) presumably because exchange between these amide protons and water moved out of the slow exchange regime, broadening the resonances beyond detection.

The importance of the state of water magnetization in NMR spectroscopy is widely recognized, and appropriate manipulation of water magnetization to achieve an improved spectral quality is well established [14,15,27]. The advantage of keeping the water magnetization unperturbed throughout the pulse sequence (e.g. SOFAST-HMQC) in comparison with the water-flip-back scheme has also been discussed in a recent review by Schanda [12]. In a recent study by Farjon et al. [28], numerical simulation predicts that hydrogen exchange in nucleic acids does not dominate the recovery of magnetization of imino protons with exchange rates <0.5 s^{-1}. Our observations of significant sensitivity gain in ^{1}H–^{15}N correlation spectra of proteins acquired with band-selective pulses for amides undergoing solvent exchange at rates ca 1–10 s^{-1} are consistent with this prediction.

While unperturbed nuclear spins (e.g. aliphatic protons) contribute to the recovery of amide ^{1}H magnetization through spin diffusion that results in a sensitivity gain in SOFAST-HMQC over conventional ^{1}H–^{15}N HSQC spectra [7,12,19], chemical exchange processes further enhance sensitivity gains for backbone amide resonances in rapid exchange with water. This exchange enhanced sensitivity gain is significant with short inter-scan delay, T_R, where an improvement in sensitivity for SOFAST-HMQC over conventional ^{1}H–^{15}N HSQC spectra up to 4-fold is observed (Fig. 3A). This substantial intensity differentiation among amide protons at shorter T_R values is quenched at T_R of ~600 ms and longer as a consequence of magnetization being averaged out among all amides protons via spin diffusion (Fig. 3A). This resultant 2-fold improvement of sensitivity at T_R > 600 ms (Fig. 3A) for SOFAST-HMQC over conventional ^{1}H–^{15}N HSQC spectra is consistent with values reported previously [29]. Recently, new SOFAST-HMQC based sequences (HET-SOFAST) making use of the hydrogen exchange phenomenon to probe structural compactness of proteins have been developed [30]. In addition, the BEST scheme has also been incorporated into many pulse sequences including the 3D heteronuclear sequences used for protein sequential assignments [31]. We expect this exchange enhanced sensitivity gain, reported here, for amide resonances in rapid exchange with water

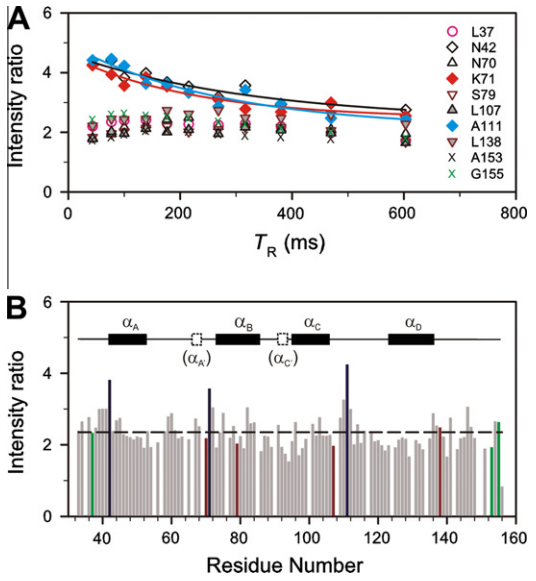

Fig. 3. Intensity ratios of SOFAST-HMQC and $^{1}H–^{15}N$ HSQC spectra showing exchange enhanced sensitivity gain for backbone amide protons in rapid exchange with water. (A) Ratios of peak intensities from the SOFAST-HMQC spectra and $^{1}H–^{15}H$ HSQC spectrum plotted against inter-scan delay, T_R, in SOFAST-HMQC for a group of residues showing significant sensitivity gains for N42, K71, and A111 relative to other amide resonances, including L37, A153 and G155 from the termini of mIL-$3_{33–156}$, which are also in exchange with water. Lines represent fitting to a three-parameter exponential decay for N42, K71, and A111, respectively. (B) Ratios of peak intensities for backbone amide resonances of mIL-$3_{33–156}$ vs. sequence position; peak intensities from the SOFAST-HMQC spectrum with T_R of 100 ms were used in the calculation. Residues shown in (A) were highlighted in (B). The dashed line in (B) represents the averaged value of the intensity ratios over all amide resonances. Also shown in (B) is a schematic of secondary structural elements of mIL-$3_{33–156}$ [22]. In both (A) and (B) the intensity ratios were calculated from their respective peak intensities from the SOFAST-HMQC and $^{1}H–^{15}N$ HSQC with intensities from the $^{1}H–^{15}N$ HSQC spectrum being scaled based on the difference in acquisition time and number of transients.

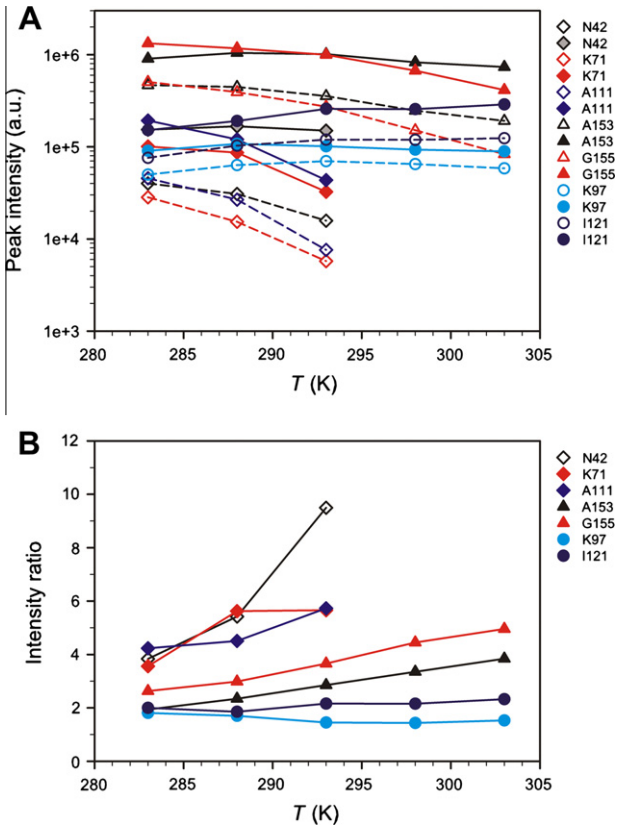

Fig. 4. Temperature dependence of intensities of $^{1}H–^{15}N$ HSQC and SOFAST-HMQC spectra and intensity ratios. (A) Temperature dependence of resonance intensities obtained from conventional $^{1}H–^{15}N$ HSQC (open symbols) and SOFAST-HMQC (closed symbols) spectra for (i) backbone amides showing temperature-dependent peak disappearance/reappearance due to significant exchange with the water (N42, K71, and A111), (ii) amides located towards the C-terminus and in exchange with the water (A153 and G155), and (iii) amides showing no noteworthy chemical exchange with the water (K97 and I121). Peak intensities from the $^{1}H–^{15}N$ HSQC were scaled down to account for different acquisition times and number of transients used in the conventional $^{1}H–^{15}N$ HSQC and SOFAST-HMQC spectra as in Fig. 3. (B) Temperature dependence of the ratio of peak intensities from $^{1}H–^{15}N$ HSQC and SOFAST-HMQC, as shown in (A), for the same group of backbone amides.

will be as significant in all applications where selective perturbation of nuclear magnetization is applied. In particular, where amide exchange processes are rapid such as in intrinsically disordered proteins there can be significant loss of backbone amide resonances at physiological pH and temperature due to increased exchange with water, as, for example, in α-synuclein [6]. Finally, this exchange enhanced sensitivity gain achievable for backbone amides in rapid exchange with water retains the sensitivity of ^{1}H nuclei when compared with heteronuclei (^{13}C) detected NMR spectroscopy [32].

3. Experimental

The NMR sample was prepared by dissolving ~1 mg lyophilized $^{13}C/^{15}N$ double-labelled mIL-$3_{33–156}$ (~1 mg) in 500 μl H_2O containing 5% $^{2}H_2O$, 20 mM potassium phosphate and 0.02% (w/v) sodium azide at pH 6.7, giving a concentration of 0.14 mM. CLEANEX spectra were recorded on a Bruker Avance 500 equipped with a cryoprobe using the CLEANEX-PM sequence [26]. The water selective shaped-pulse was a 7.5 ms Gaussian. All spectra were acquitted with 1024 and 64 complex data points over spectral widths of 12.0 and 32.0 ppm for F2 (^{1}H) and F1 (^{15}N), respectively, with 128 transients and an inter-scan delay T_R of 1.2 s. The following equation is used to fit the exchange rate, k:

$$V/V_0 = [k/(R_{1A} + k - R_{1B})]\{\exp(-R_{1B}\tau_m) - \exp[-(R_{1A} + k)\tau_m]\} \quad (1)$$

where R_{1A} is the relaxation rate of the nuclear spin in exchange with the solvent under the CLEANEX mixing condition (a combination of transverse and longitudinal relaxation), R_{1B} is the water relaxation rate during the CLEANEX mixing time, τ_m, and k is the exchange rate. V and V_0 are peak volumes from CLEANEX spectra at various mixing times and a reference $^{1}H–^{15}N$ HSQC spectrum, respectively [26].

Both sensitivity-enhanced, water-flip-back HSQC [14] and SOFAST-HMQC [7] spectra were recorded on a Bruker DRX600 spectrometer equipped with triple-resonance inverse TXI probe using standard pulse standard sequences. For SOFAST-HMQC the shaped pulse for ^{1}H excitation was a polychromatic PC9 of 3 ms with a rotation angle of 120°, and the subsequent band-selective ^{1}H refocusing pulse is an r-SNOB with duration of 1 ms as in the original sequence [7]. Offsets for both shaped-pulses PC9 and r-SNOB are 8.15 ppm. Both $^{1}H–^{15}N$ HSQC and SOFAST-HMQC spectra were acquired with 256 and 64 complex data points over spectral widths of 12.0 and 32.0 ppm for F2 (^{1}H) and F1 (^{15}N), respectively, with ^{13}C decoupling in the F1(^{15}N) dimension achieved with a 500 μs Chirp pulse. For SOFAST-HMQC spectra recorded at different T_R values, the number of transients was adjusted (ranging from 16 to 96) to keep the total acquisition time for each spectrum fixed at 23 min and 14 s. Intensity ratios were calculated from their respective peak intensities from the SOFAST-HMQC and $^{1}H–^{15}N$ HSQC with intensities from the $^{1}H–^{15}N$ HSQC spectrum being scaled based on the difference in acquisition time and number of transients

(i.e. normalized to the background noise). All spectra were processed using TOPSPIN (Bruker BioSpin) and analyzed with XEASY software [33].

Acknowledgments

This work was supported in part by the National Health and Medical Research Council (NHMRC), Australia (Program Grant 461219). Fellowship support was provided by the NHMRC (J.M.M., R.S.N.) and Australian Research Council (Grant FT100100100 to J.M.M). The authors would like to thank Dr. Christopher MacRaild for helpful discussions.

References

[1] Z. Kuang, S. Yao, K.A. McNeil, B.E. Forbes, J.C. Wallace, R.S. Norton, Insulin-like growth factor-I (IGF-I): solution properties and NMR chemical shift assignments near physiological pH, Growth Horm. IGF Res. 19 (2009) 226–231.
[2] A. Zhuravleva, V.Y. Orekhov, Divided evolution: a scheme for suppression of line broadening induced by conformational exchange, J. Am. Chem. Soc. 130 (2008) 3260–3261.
[3] Y. Li, A.G. Palmer, Narrowing of protein NMR spectral lines broadened by chemical exchange, J. Am. Chem. Soc. 132 (2010) 8856–8857.
[4] S.T. Hsu, C.W. Bertoncini, C.M. Dobson, Use of protonless NMR spectroscopy to alleviate the loss of information resulting from exchange-broadening, J. Am. Chem. Soc. 131 (2009) 7222–7223.
[5] A.G. Palmer, NMR characterization of the dynamics of biomacromolecules, Chem. Rev. 104 (2004) 3623–3640.
[6] R.L. Croke, C.O. Sallum, E. Watson, E.D. Watt, A.T. Alexandrescu, Hydrogen exchange of monomeric α-synuclein shows unfolded structure persists at physiological temperature and is independent of molecular crowding in *Escherichia coli*, Protein Sci. 17 (2008) 1434–1445.
[7] P. Schanda, B. Brutscher, Very fast two-dimensional NMR spectroscopy for real-time investigation of dynamic events in proteins on the time scale of seconds, J. Am. Chem. Soc. 127 (2005) 8014–8015.
[8] L. Frydman, T. Scherf, A. Lupulescu, The acquisition of multidimensional NMR spectra within a single scan, Proc. Natl. Acad. Sci. U.S.A. 99 (2002) 15858–15862.
[9] D. Rovnyak, D.P. Frueh, M. Sastry, Z.Y. Sun, A.S. Stern, J.C. Hoch, G. Wagner, Accelerated acquisition of high resolution triple-resonance spectra using non-uniform sampling and maximum entropy reconstruction, J. Magn. Reson. 170 (2004) 15–21.
[10] Ē. Kupče, R. Freeman, Projection–reconstruction technique for speeding up multidimensional NMR spectroscopy, J. Am. Chem. Soc. 126 (2004) 6429–6440.
[11] D. Malmodin, M. Billeter, High-throughput analysis of protein NMR spectra, Prog. NMR Spectrosc. 46 (2005) 109–129.
[12] P. Schanda, Fast-pulsing longitudinal relaxation optimized techniques: enriching the toolbox of fast biomolecular NMR spectroscopy, Prog. NMR Spectrosc. 55 (2009) 238–265.
[13] P. Schanda, H. Van Melckebeke, B. Brutscher, Speeding up three-dimensional protein NMR experiments to a few minutes, J. Am. Chem. Soc. 128 (2006) 9042–9043.
[14] S. Grzesiek, A. Bax, The importance of not saturating H_2O in protein NMR. Application to sensitivity enhancement and NOE measurements, J. Am. Chem. Soc. 115 (1993) 12593–12594.
[15] T. Diercks, M. Daniels, R. Kaptein, Extended flip-back schemes for sensitivity enhancement in multidimensional HSQC-type out-and-back experiments, J. Biomol. NMR 33 (2005) 243–259.
[16] K. Pervushin, B. Vogeli, A. Eletsky, Longitudinal ^{1}H relaxation optimization in TROSY NMR spectroscopy, J. Am. Chem. Soc. 124 (2002) 12898–12902.
[17] A. Abragam, The Principles of Nuclear Magnetism, Clarendon Press, Oxford, 1961.
[18] A.D. Bain, Chemical exchange in NMR, Prog. NMR Spectrosc. 43 (2003) 63–103.
[19] M. Deschamps, I.D. Campbell, Cooling overall spin temperature: protein NMR experiments optimized for longitudinal relaxation effects, J. Magn. Reson. 178 (2006) 206–211.
[20] J.M. Murphy, D. Metcalf, I.G. Young, D.J. Hilton, A convenient method for preparation of an engineered mouse interleukin-3 analog with high solubility and wild-type bioactivity, Growth Factors 28 (2010) 104–110.
[21] S. Yao, J.M. Murphy, A. Low, R.S. Norton, ^{1}H, ^{13}C and ^{15}N resonance assignments of a highly-soluble murine interleukin-3 analogue with wild-type bioactivity, Biomol. NMR Assign. 4 (2010) 73–77.
[22] S. Yao, I.G. Young, R.S. Norton, J.M. Murphy, Murine interleukin-3: structure, dynamics and conformational heterogeneity in solution, Biochemistry 50 (2011) 2464–2477.
[23] N.J. Baxter, L.L. Hosszu, J.P. Waltho, M.P. Williamson, Characterisation of low free-energy excited states of folded proteins, J. Mol. Biol. 284 (1998) 1625–1639.
[24] M. Roy, L.L. Chavez, J.M. Finke, D.K. Heidary, J.N. Onuchic, P.A. Jennings, The native energy landscape for interleukin-1β. Modulation of the population ensemble through native-state topology, J. Mol. Biol. 348 (2005) 335–347.
[25] R.F. Latypov, D. Liu, K. Gunasekaran, T.S. Harvey, V.I. Razinkov, A.A. Raibekas, Structural and thermodynamic effects of ANS binding to human interleukin-1 receptor antagonist, Protein Sci. 17 (2008) 652–663.
[26] T.L. Hwang, P.C. van Zijl, S. Mori, Accurate quantitation of water–amide proton exchange rates using the phase-modulated CLEAN chemical exchange (CLEANEX-PM) approach with a Fast-HSQC (FHSQC) detection scheme, J. Biomol. NMR 11 (1998) 221–226.
[27] S. Hiller, G. Wider, T. Etezady-Esfarjani, R. Horst, K. Wüthrich, Managing the solvent water polarization to obtain improved NMR spectra of large molecular structures, J. Biomol. NMR 32 (2005) 61–70.
[28] J. Farjon, J. Boisbouvier, P. Schanda, A. Pardi, J.-P. Simorre, B. Brutscher, Longitudinal-relaxation-enhanced NMR experiments for the study of nucleic acids in solution, J. Am. Chem. Soc. 131 (2009) 8571–8577.
[29] P. Schanda, Ē. Kupče, B. Brutscher, SOFAST-HMQC experiments for recording two-dimensional heteronuclear correlation spectra of proteins within a few seconds, J. Biomol. NMR 33 (2005) 199–211.
[30] P. Schanda, V. Forge, B. Brutscher, HET-SOFAST NMR for fast detection of structural compactness and heterogeneity along polypeptide chains, Magn. Reson. Chem. 44 (2006) S177–S184.
[31] E. Lescop, P. Schanda, B. Brutscher, A set of BEST triple-resonance experiments for time-optimized protein resonance assignment, J. Magn. Reson. 187 (2007) 163–169.
[32] W. Bermel, I. Bertini, I.C. Felli, M. Piccioli, R. Pierattelli, ^{13}C-detected protonless NMR spectroscopy of proteins in solution, Prog. NMR Spectrosc. 48 (2006) 25–45.
[33] C. Bartels, T.H. Xia, M. Billeter, P. Güntert, K. Wüthrich, The program XEASY for computer-supported NMR spectral-analysis of biological macromolecules, J. Biomol. NMR 6 (1995) 1–10.